Study of η photoproduction on the proton in a chiral constituent quark approach via one-gluon-exchange model

Jun He,[1,*] B. Saghai,[1,†] and Zhenping Li[2]

[1] *Institut de Recherche sur les lois Fondamentales de l'Univers, DSM/IRFU, CEA/Saclay, 91191 Gif-sur-Yvette, France*

[2] *Department of Computer and Information Science, University of Maryland, MD 20783, USA*

(Dated: February 26, 2008)

Abstract

A formalism based on a chiral quark model (χQM) approach complemented with a one-gluon exchange model, to take into account the breakdown of the $SU(6) \otimes O(3)$ symmetry, is presented. The configuration mixing of wave functions for nucleon and resonances are derived. With few adjustable parameters, differential cross-section and polarized beam asymmetry for the $\gamma\, p \,\rightarrow\, \eta\, p$ process are calculated and successfully compared with the data in the centre-of-mass energy range from threshold up to 2 GeV. The known resonances $S_{11}(1535)$, $S_{11}(1650)$, $P_{13}(1720)$, $D_{13}(1520)$, and $F_{15}(1680)$, as well as two new S_{11} and D_{15} resonances are found to be dominant in the reaction mechanism. Besides, connections among the scattering amplitudes of the χQM approach and the helicity amplitudes, as well as decay widths of resonances are established. Possible contributions from the so-called "missing resonances" are investigated and found to be negligible.

PACS numbers: 13.60.Le, 12.39.Fe, 12.39.Jh, 14.20.Gk

*jun.he@cea.fr

†bijan.saghai@cea.fr

I. INTRODUCTION

Electromagnetic production of mesons on the nucleon offers a great opportunity to deepen our understanding of the baryon resonances properties. In recent years, intensive experimental efforts have been devoted to the measurement of observables for the processes of pseudoscalar and vector mesons production, using electron and/or photon beam facilities.

In the present work we investigate the reaction $\gamma\ p\ \rightarrow\ \eta\ p$, in the range of centre-of-mass total energy from threshold up to $W\ \approx 2$ GeV, in order to interpret a large amount of high quality data released from various facilities, namely, differential cross-section data by the following collaborations: MAMI [1], CLAS [2], CB-ELSA [3], LNS-GeV-γ [4] and GRAAL [5], polarized beam asymmetries by CB-ELSA/TAPS [6] and GRAAL [5].

The copious set of data has motivated extensive theoretical investigations. Most of the available models are based on meson-nucleon degrees of freedom, in which the Feynman diagrammatic techniques are used, so that the transition amplitudes are Lorentz invariant. In recent years various advanced approaches have been developed, namely, the unitary isobar model of MAID [7], Geissen [8] and Bonn-Gatchina groups [9] coupled-channel approaches, as well as the partial wave analysis of SAID [10]. Those approaches have no explicit connection with QCD, and the number of parameters in the models increases with the number of resonances included in the models.

Formalisms embodying the subnucleonic degrees of freedom are also being developed. Such a program has its genesis in the early works by Copley, Karl and Obryk [11] and Feynman, Kisslinger and Ravndal [12] in the pion photoproduction, who provided the first clear evidence of the underlying $SU(6)\otimes O(3)$ structure of the baryon spectrum. The subsequent works [13, 14] in the framework of the constituent quark models concentrated mainly on the transition amplitudes and the baryon mass spectrum, predicting still undiscovered or "missing", resonances. However, those approaches did not investigate reaction mechanisms.

In Ref. [15] a comprehensive and unified approach to the pseudoscalar mesons photoproduction, based on the low energy QCD Lagrangian [16], is developed with the explicit quark degrees of freedom. This approach reduces drastically the number of free parameters, for example, within the exact $SU(6)\otimes O(3)$ symmetry, the reaction under investigation has only one free parameter, namely, ηNN coupling constant. However, that symmetry is broken and in order to take into account that effect, one free parameter per resonance was introduced in

previous calculations [17, 18]. Given that the configuration mixing among the 3-constituent quarks bound states is a consequence of the $SU(6) \otimes O(3)$ symmetry breakdown, in the present work we use the one-gluon-exchange mechanism to generate the configuration mixing of the wave functions. In this approach, the number of parameters decreases significantly. After the parameters are determined by fitting the data, we then study the contributions from the missing resonances (see e.g. Refs. [19–21]). Besides, we give relations connecting the scattering amplitudes in our χQM approach to the photoexcitation helicity amplitudes and partial decay widths of resonances. Our approach offers also the opportunity of investigating new nucleon resonances, for which strong indications have been reported in the literature [9, 18, 22–31].

The paper is organized as follows. In Section II, the theoretical content of our work is presented. Starting from a chiral effective Lagrangian, the CGLN amplitudes for the process $\gamma\ p \ \rightarrow \ \eta\ p$ are given within the $SU(6) \otimes O(3)$ symmetry. Then the consequences of the breaking of that symmetry *via* configuration mixing in One-Gluon-Exchange (OGE) model is reported and helicity amplitudes of photon transition and meson decay partial widths of resonances are presented. The fitting procedure and numerical results for differential cross-section, polarized beam asymmetry, helicity amplitudes, and $N^* \ \rightarrow \ \eta\ N$ partial decay width are reported and discussed in Section III, where possible roles played by new / missing resonances are examined. Summary and conclusions are given in Section IV.

II. THEORETICAL FRAME

In this Section we recall the content of a chiral constituent quark approach and relate it to the configuration mixing of constituent quarks states *via* a OGE model, generated by the breakdown of the $SU(6) \otimes O(3)$ symmetry. Then we present issues related to the photoexcitation helicity amplitudes and the partial decay widths of nucleon resonances.

A. Chiral constituent quark model

As in Ref. [15] we start from an effective chiral Lagrangian [16],

$$\mathcal{L} = \bar{\psi}[\gamma_\mu(i\partial^\mu + V^\mu + \gamma_5 A^\mu) - m]\psi + \cdots, \tag{1}$$

where vector (V^μ) and axial (A^μ) currents read,

$$V^\mu = \frac{1}{2}(\xi\partial^\mu\xi^\dagger + \xi^\dagger\partial^\mu\xi) \ , \ A^\mu = \frac{1}{2i}(\xi\partial^\mu\xi^\dagger - \xi^\dagger\partial^\mu\xi), \tag{2}$$

with $\xi = \exp(i\phi_m/f_m)$ and f_m the meson decay constant. ψ and ϕ_m are the quark and meson fields, respectively.

There are four components for the photoproduction of pseudoscalar mesons based on the QCD Lagrangian,

$$\begin{aligned}\mathcal{M}_{fi} \ = \ \langle N_f|H_{m,e}|N_i\rangle + \sum_j \Big\{ & \frac{\langle N_f|H_m|N_j\rangle\langle N_j|H_e|N_i\rangle}{E_i+\omega-E_j} + \\ & \frac{\langle N_f|H_e|N_j\rangle\langle N_j|H_m|N_i\rangle}{E_i-\omega_m-E_j}\Big\} + \mathcal{M}_T,\end{aligned} \tag{3}$$

where $N_i(N_f)$ is the initial (final) state of the nucleon, and $\omega(\omega_m)$ represents the energy of incoming (outgoing) photons (mesons). The first term in Eq. (3) is a seagull term. It is generated by the gauge transformation of the axial vector A_μ in the QCD Lagrangian. This term, being proportional to the electric charge of the outgoing mesons, does not contribute to the production of the η-meson. The second and third terms correspond to the s- and u-channels, respectively. The last term is the t-channel contribution.

In this paper we focus on the nucleon resonance contributions. Given that the u-channel contributions are less sensitive to the details of resonances structure than those in the s--channel, it is then reasonable to treat the u-channel components as degenerate [18].

For s-channel, the amplitudes are given by the following expression [15, 18]:

$$\mathcal{M}_{N^*} = \frac{2M_{N^*}}{s - M_{N^*}^2 - iM_{N^*}\Gamma(\mathbf{q})} e^{-\frac{\mathbf{k}^2+\mathbf{q}^2}{6\alpha^2}} \mathcal{O}_{N^*}, \tag{4}$$

where $\sqrt{s} \ \equiv \ W \ = \ E_N + \omega_\gamma = E_S + \omega_m$ is the total centre-of-mass energy of the system, and $\mathcal{O}_{N^*}$ is determined by the structure of each resonance. $\Gamma(\mathbf{q})$ in Eq. (4) is the total width of the resonance, and a function of the final state momentum $\mathbf{q}$.

The transition amplitude for the n^{th} harmonic-oscillator shell is

$$\mathcal{O}_n = \mathcal{O}_n^2 + \mathcal{O}_n^3. \tag{5}$$

The first (second) term represents the process in which the incoming photon and outgoing meson, are absorbed and emitted by the same(different) quark.

In the present work, we use the standard multipole expansion of the CGLN amplitudes [32], and obtain the partial wave amplitudes of resonance $l_{2I,2l\pm1}$. Then, the transition amplitude takes the following form:

$$\mathcal{O}_{N^*} = if_{1l\pm}\sigma\cdot\epsilon + f_{2l\pm}\sigma\cdot\hat{\mathbf{q}}\sigma\cdot(\hat{\mathbf{k}}\times\epsilon) + if_{3l\pm}\sigma\cdot\hat{\mathbf{k}}\hat{\mathbf{q}}\cdot\epsilon + if_{4l\pm}\sigma\cdot\hat{\mathbf{q}}\epsilon\cdot\hat{\mathbf{q}}. \tag{6}$$

Expressing the CGLN amplitudes in their usual formulation [33, 34], leads to the Hebb-Walker amplitudes in terms of photoexcitation helicity amplitudes,

$$A_{l\pm} = \mp f A^{N^*}_{1/2}, \tag{7}$$

$$B_{l\pm} = \pm f\sqrt{\frac{4}{l(l+2)}}A^{N^*}_{3/2}, \tag{8}$$

where

$$f = \frac{1}{(2J+1)2\pi}[\frac{M_N E_N}{M^2_{N^*}}k]^{1/2}\frac{2M_{N^*}}{s-M^2_{N^*}+iM_{N^*}\Gamma(q)}A^m_{1/2} \equiv f_0\frac{2M_{N^*}}{s-M^2_{N^*}+iM_{N^*}\Gamma(q)}, \tag{9}$$

with $A^m_{1/2}$ the $N^* \to \eta N$ decay amplitude, appearing in the partial decay width,

$$\Gamma_m = \frac{1}{(2J+1)}\frac{|\mathbf{q}|E_N}{\pi M_{N^*}}|A^m_{1/2}/C^I_{mN}|^2, \tag{10}$$

where $C^I_{\pi N}$ represents the Clebsch-Gordan coefficients related to the isospin coupling in the outgoing channel.

In Ref. [15], the partial decay amplitudes are used to separate the contribution of the state with the same orbital angular momentum L. In fact, with the helicity amplitudes of photon transition and meson decay we can directly obtain the CGLN amplitudes for each resonances in terms of Legendre polynomials derivatives:

$$\begin{aligned}
f_{1l\pm} &= f_0[\mp A^{N^*}_{1/2} - \sqrt{\frac{l+1/2\mp1/2}{l+1/2\pm3/2}}A^{N^*}_{3/2}]P'_{\ell\pm1}, \\
f_{2l\pm} &= f_0[\mp A^{N^*}_{1/2} - \sqrt{\frac{l+1/2\pm3/2}{l+1/2\mp\ 1/2}}A^{N^*}_{3/2}]P'_{\ell}, \\
f_{3l\pm} &= \pm f_0\frac{2A^{N^*}_{3/2}}{\sqrt{(l-1/2\pm1/2)(l+3/2\pm1/2)}}P''_{\ell\pm1}, \\
f_{4l\pm} &= \mp f_0\frac{2A^{N^*}_{3/2}}{\sqrt{(l-1/2\pm1/2)(l+3/2\pm\ 1/2)}}P''_{\ell}.
\end{aligned} \tag{11}$$

All f_is are proportional to the meson decay amplitudes. So they can be used to separate the contributions from the state with the same N and L as presented in Ref. [15].

In our approach, the photoexcitation helicity amplitudes $A^{N^*}_{1/2}$ and $A^{N^*}_{3/2}$, as well as the decay amplitudes, are related to the matrix elements of the electromagnetic interaction Hamiltonian [11],

$$A_\lambda = \sqrt{\frac{2\pi}{k}}\langle N^*; J\lambda|H_e|N; \frac{1}{2}\lambda - 1\rangle, \tag{12}$$

$$A^m_\nu = \langle N; \frac{1}{2}\nu|H_m|N^*; J\nu\rangle. \tag{13}$$

B. Configuration Mixing

The amplitudes in Sec.II A are derived under the $SU(6)\otimes O(3)$ symmetry. However, for physical states that symmetry is broken. An example is the violation of the Moorhouse rule [35]. In Ref. [17], a set of parameters C_{N^*} were hence introduced to take into account the breaking of that symmetry, *via* following substitution:

$$\mathcal{O}_{N^*} \to C_{N^*}\mathcal{O}_{N^*}. \tag{14}$$

In Refs. [17, 18], those parameters were allowed to vary around their $SU(6)\otimes O(3)$ values ($|C_{N^*}| = 0$ or 1). In this work, instead of using those adjustable parameters, we introduce the breakdown of that symmetry through the configuration mixings of baryons wave functions.

To achieve such an improvement, we must choose a potential model. The popular used ones are one-gluon-exchange (OGE) model [36–38] and Goldstone boson exchange model [39]. As shown in Refs. [40, 41], these two models give similar mixing angles for the negative parity resonances and the relevant observables. Here, we adopt the OGE model which has been successfully used to study the helicity amplitudes and decay widths [13] of resonances.

In OGE model, the Hamiltonian of system can be written as [36–38],

$$H = \sum_{i=1}^{3} m_i + \sum_{i=1}^{3}\frac{p_i^2}{2m_i^2} + \sum_{i<j=1}^{3}\tfrac{1}{2}Kr_{ij}^2 + \sum_{i<j=1}^{3}U(r_{ij}) + H_{hyp}\ , \tag{15}$$

where the m_i is the "constituent" effective masse of quark i and $r_{ij} = r_i - r_j$ the separation between two quarks. The confinement potential has two components; one written as a harmonic oscillator potential ($\frac{1}{2}Kr_{ij}^2$, with K the spring constant), and an unspecified anharmonicity $U(r_{ij})$, treated as a perturbation.

The hyperfine part interaction is the sum of contact and tensor terms,

$$H_{hyp} = \frac{2\alpha_s}{3m_q^2} \sum_{i<j=1}^{3} \left\{ \frac{8\pi}{3} \mathbf{S}_i \cdot \mathbf{S}_j \ \ \delta^3(\mathbf{r}_{ij}) + \frac{1}{r_{ij}^3}(\frac{3\mathbf{S}_i \cdot \mathbf{r}_{ij} \ \mathbf{S}_j \cdot r_{ij}}{\mathbf{r}_{ij}^2} - \mathbf{S}_i \cdot \mathbf{S}_j) \right\}. \qquad (16)$$

Here, $\mathbf{S}_i$ is the spin of quark i, and α_s a normalization factor, treated as free parameter [38].

The hyperfine interaction generates the configuration mixings among the ground-state N^2S_S ($[56, O^+]$) and other configurations, e.g. $N^2S'_S$ ($[56', O^+]$), N^2S_M ($[70, O^+]$), and N^4D_M ($[70, 2^+]$). Here, the notation is $X^{2S+1}L_\pi$, where $X = N,\ \Delta,\ \Sigma, ...,\ S$ the total quark spin, $L = S,\ P,\ D...$ the total orbital angular momentum, and $\pi = S,\ M$ or A the permutational symmetry (symmetric, mixed symmetry, or antisymmetric, respectively) of spatial wave function.

The first two terms in Eq. (15) can be rewritten as two harmonic oscillators within the Jocabi coordinate. Its solution is the well known $SU(6) \otimes O(3)$ wave functions. The breakdown of the symmetry arises from the additional terms. Given that the configuration mixing is mainly produced by the spin- and flavor-dependent parts of Hamiltonian [40], here we use a simple method to deal with the confinement terms in Refs. [19, 37], where three constants E_0, Ω, and Δ are introduced.

In order to illustrate the modifications of the scattering amplitudes due to the $SU(6) \otimes O(3)$ symmetry breakdown, we give in the following the explicit derivations in the case of the $S_{11}(1535)$ resonance . In lines with Ref. [18], we express the amplitudes $\mathcal{A}_{S_{11}}$ in terms of the product of the photoexcitation and meson-decay transition amplitudes,

$$\mathcal{A}_{S_{11}} \propto < N|H_m|S_{11} >< S_{11}|H_e|N >, \qquad (17)$$

where H_m and H_e are the meson and photon transition operators, respectively. The wave function can be written within the $SU(6) \otimes O(3)$ symmetry for $n \leq 2$ shells as $X^{2S+1}L_\pi J^P$ and configuration mixings, with J^P the state's total angular momentum and parity,

$$|S_{11}(1535)\rangle = -\sin\theta_S |N^4P_M \tfrac{1}{2}^-\rangle + \cos\theta_S |N^2P_M \tfrac{1}{2}^-\rangle, \qquad (18)$$

$$|Nucleon\rangle = c_1|N^2S_S\tfrac{1}{2}^+\rangle + c_2|N^2S'_S\tfrac{1}{2}^+\rangle + c_3|N^4D_M\tfrac{1}{2}^+\rangle + c_4|N^2S_M\tfrac{1}{2}^+\rangle + c_5|N^2P_A\tfrac{1}{2}^+\rangle, \qquad (19)$$

where θ_S and c_i can be determined by the OGE model. If we set $c_1 = 1$ and $c_{2,3,4,5} = 0$ (so $\theta_S = 0$), then, the $SU(6) \otimes O(3)$ symmetry is restored. The improvement compared

to Ref. [18] is that here we not only take into account the mixing in the intermediate S_{11} resonance but also in the initial- and final-state nucleon. Moreover, for other resonances, we also include directly the configuration mixing of wave functions *via* OGE model, so that we do not need to introduce the free parameters C_{N^*} (Eq. (14)).

The electromagnetic transition amplitudes then take the following form:

$$\begin{aligned} < S_{11}|H_e|N > &= c_1 < S_{11}|H_e|N^2 S_S \tfrac{1}{2}^+\rangle + c_2 < S_{11}|H_e|N^2 S'_S \tfrac{1}{2}^+\rangle + c_3 < S_{11}|H_e|N^4 D_M \tfrac{1}{2}^+\rangle \\ &+ c_4 < S_{11}|H_e|N^2 S_M \tfrac{1}{2}^+\rangle + c_5 < S_{11}|H_e|N^2 P_A \tfrac{1}{2}^+\rangle \\ &= c_1 \cos\theta < N^2 P_M \tfrac{1}{2}^-|H_e|N^2 S_S \tfrac{1}{2}^+\rangle + ... \end{aligned} \tag{20}$$

Here, the term $< N^4 P_M \frac{1}{2}^-|H_e|N^2 S_S \frac{1}{2}^+\rangle$ vanishes because of the Moorhouse rule [35]. In Ref. [18], the mixing angles are introduced also to give a nonzero value for contributions from the $D_{13}(1700)$ resonance, but the nucleon wave function includes only the $n = 0$ part, that is, $c_1 = 1$, $c_{2,3,4,5} = 0$. Moreover, the contribution of the $D_{15}(1675)$ ($|N^4 D_M \frac{5}{2}^+\rangle$ state) is zero, if we consider only the wave function up to $n = 2$. Then, in Ref. [18], for this latter resonance a term identical to the contribution to the η photoproduction on neutron target was added by hands. In this work, the nucleon wave function with $n = 2$ produces *naturally* a non-zero contribution with the same form as for neutron target under the $SU(6) \otimes O(3)$ symmetry.

Analogously, for meson decay amplitudes we get,

$$< N|H_m|S_{11} > = c_1(\cos\theta_S - \mathcal{R}\sin\theta_S) < N^2 S_S \tfrac{1}{2}^+|H_m|N^2 P_M \tfrac{1}{2}^-\rangle + ... \tag{21}$$

and the ratio

$$\mathcal{R} = \frac{< N|H_m|N(^4P_M)_{\frac{1}{2}^-} >}{< N|H_m|N(^2P_M)_{\frac{1}{2}^-} >}, \tag{22}$$

is a constant determined by the $SU(6) \otimes O(3)$ symmetry.

Then, Eq. (17) reads,

$$\mathcal{A}_{S_{11}} = C_{S_{11}} < N^2 S_S \tfrac{1}{2}^+|H_m|N^2 P_M \tfrac{1}{2}^- >< N^2 P_M \tfrac{1}{2}^-|H_e|N^2 S_S \tfrac{1}{2}^+ > +..., \tag{23}$$

where,

$$C_{S_{11}} = c_1^2(\cos^2\theta_S - \mathcal{R}\sin\theta_S\cos\theta_S) + ... \tag{24}$$

So, if we remove all $n = 2$ parts from the wave function of the nucleon, as in Ref. [17], then the factor $C_{S_{11}}$ is a constant. However after other contributions are included, it becomes dependent on the momenta k and q. In this work we keep this dependence.

III. RESULTS AND DISCUSSION

With the formalism presented in Sec.II, we investigate the process $\gamma p \to \eta p$. A chiral constituent quark model was proven [18] to be an appropriate approach to that end. That work embodied one free parameter per nucleon resonance, in order to take into account the breaking of the $SU(6) \otimes O(3)$ symmetry. In the present work, this latter phenomenon is treated via configuration mixing, reducing the number of adjustable parameters. As in Refs. [18], we introduce resonances in $n \leq 2$ shells, to study the η photoproduction in the centre-of-mass energy $W \leq 2$ GeV.

A. Fitting procedure

Using the CERN MINUIT code, we have fitted simultaneously the following data sets:

- **Differential cross-section:** Data base includes 1220 data points, for $1.49 \lesssim W \leq 1.99$ GeV, coming from the following labs: MAMI [1], CLAS [2], ELSA [3], LNS [4], and GRAAL [5]. Only statistical uncertainties are used.

- **Polarized beam asymmetry:** Polarized beam asymmetries (184 data points), for $1.49 \lesssim W \leq 1.92$ GeV, from GRAAL [5] and ELSA [6]. Only statistical uncertainties are used.

- **Spectrum of known resonances:** For spectrum of known resonances, we use as input their PDG values [42] for masses and widths, with the uncertainties reported there plus an additional theoretical uncertainty of 15 MeV, as in Ref. [14], in order to avoid overemphasis of the resonances with small errors. The data base contains all 12 known nucleon resonances as in PDG, with $M \leq 2$ GeV, namely,

  ***n*=1:** $S_{11}(1535)$, $S_{11}(1650)$, $D_{13}(1520)$, $D_{13}(1700)$, and $D_{15}(1675)$;

  ***n*=2:** $P_{11}(1440)$, $P_{11}(1710)$, $P_{13}(1720)$, $P_{13}(1900)$, $F_{15}(1680)$, $F_{15}(2000)$, and $F_{17}(1990)$.

  Besides the above isospin-1/2 resonances, we fitted also the mass of $\Delta(1232)$ resonance. However, spin-3/2 resonances do not intervene in the η photoproduction.

- **Additional resonance:** Resonances with masses above $M \approx 2$ GeV, treated as degenerate, are simulated by a single resonance, for which are left as adjustable parameters the mass, the width, and the symmetry breaking coefficient.

The adjustable parameters, listed in Table I, are as follows: η nucleon coupling ($g_{\eta NN}$), mass of the non-strange quarks (m_q), harmonic oscillator strength (α), QCD coupling constant (α_s), confinement constants (E_0, Ω, and Δ), three parameters M, Γ, and C_N^* related to the degenerate treatment of resonances with masses above ≈ 2 GeV, and the strength of the $P_{13}(1720)$ resonance. We will come back to this latter parameter.

The spectrum of the known resonances put constraints on six of the adjustable parameters. Five of them (m_q, α, α_s, Ω, and Δ) are determined through an interplay between the mass spectrum of the resonances and the photoproduction data *via* the configurations mixings parameters c_i (Eq. 20). The sixth one, E_0, is determined by the mass of nucleon. The coupling constant $g_{\eta NN}$ is determined by photoproduction data. The parameter $C_{P_{13}(1720)}$ is the strength of the $P_{13}(1720)$ resonance, that we had to leave as a free parameter in order to avoid its too large contribution resulting from direct calculation. This latter parameter, as well as those defining the higher mass resonance (HM N^*) are determined by the photoproduction data. Notice that in fitting the photoproduction data, we use the PDG [42] values for masses and widths of resonances.

The complete set of adjustable parameters mentioned above, leads to our model A (see 3^{rd} column in Table I for which the reduced χ^2 turns out to be large (12.37).

In recent years, several authors [9, 18, 22–31] have put forward need for new resonances in interpreting various observables, with extracted masses roughly between 1.73 and 2.1 GeV. We have hence, investigated possible contributions from three of them: S_{11}, D_{13}, and D_{15}. For each of those new resonances we introduce then three additional adjustable parameters per resonance: mass (M), width (Γ), and symmetry breaking coefficient (C_{N^*}). Fitting the same data base, we obtained a second model, called model B, for which the adjustable parameters are reported in the last column of Table I. The reduced χ^2 is very significantly improved going down from 12.37 to 2.31. In the rest of this Section, we concentrate on the model B.

Extracted values within OGE model come out close to those used by Isgur and Capstick [19, 37]: $E_0 = 1150$ MeV, $\Omega \approx 440$ MeV, $\Delta \approx 440$ MeV. For three other parameters,

TABLE I: Adjustable parameters and their extracted values, with m_q, α, E_0, Ω, Δ, M, and Γ in MeV.

	Parameter	Model A	Model B
	$g_{\eta NN}$	0.391	0.449
	m_q	277	304
	α	288	285
	α_s	1.581	1.977
	E_0	1135	1138
	Ω	450	442
	Δ	460	460
	$C_{P_{13}(1720)}$	0.382	0.399
HM N^*:			
	M	1979	2129
	Γ	124	80
	C_{N^*}	-0.85	-0.70
New S_{11}:			
	M		1717
	Γ		217
	C_{N^*}		0.59
New D_{13}:			
	M		1943
	Γ		139
	C_{N^*}		-0.19
New D_{15}:			
	M		2090
	Γ		328
	C_{N^*}		2.89
$\chi^2_{d.o.f}$		12.37	2.31

Isgur and Capstick introduce $\delta = (4\alpha_s\alpha)/(3\sqrt{2\pi}m_u^2)$, for which they get ≈ 300 MeV. Model B gives $\delta \approx 262$ MeV.

For the three new resonances, we follow the method in Ref. [17], as discussed in Sec.II B, *via* Eq. (14). The extracted Wigner mass and width, as well as the strength for those resonances are given in Table I.

For the new S_{11}, the Wigner mass and width are consistent with the values in Refs. [18, 22, 23, 31], but the mass is lower, by about 100 to 200 MeV, than findings by other authors [24, 26–28, 43]. The most natural explanation would be that it is the first S_{11} state in the $n = 3$ shell, however its low mass could indicate a multiquark component, such as, a quasi-bound kaon-hyperon [22] or a pentaquark state [44]. For the $D_{13}(1850)$, the variation of χ^2 is small. Interestingly, we find large effect from a D_{15} state around 2090 GeV with a Wigner width of 330 MeV. It is very similar to the $N(2070)D_{15}$ reported in Refs. [3, 9]. It can be explained as the first D_{15} state in $n = 3$ shell [3].

The results of baryon spectrum extracted from the present work are reported in Tables II and III. Table II is devoted to the known resonances. Our results are in good agreement with those obtained by Isgur and Karl [37, 38], and except for the $S_{11}(1535)$ and $D_{13}(1520)$, fall in the ranges estimated by PDG [42]. The additional "missing" resonances generated by the OGE model, are shown in Table III. The extracted masses are compatible with those reported by Isgur and Karl [37, 38].

TABLE II: Extracted masses for known resonances. For each resonance, results of the present work (M^{OGE}) are given in the first line, predictions from Isgur and Karl for negative-parity [38] and positive-parity [37] excited baryons in the second line, and PDG values [42] in the third line.

	$S_{11}(1535)$	$S_{11}(1650)$	$P_{11}(1440)$	$P_{11}(1710)$	$P_{13}(1720)$	$P_{13}(1900)$
M^{OGE}	1473	1620	1428	1723	1718	1854
Refs. [37, 38]	1490	1655	1405	1705	1710	1870
M^{PDG}	1535 ± 10	1655^{+15}_{-10}	1440^{+30}_{-20}	1710 ± 30	1720^{+30}_{-20}	1900
	$D_{13}(1520)$	$D_{13}(1700)$	$D_{15}(1675)$	$F_{15}(1680)$	$F_{15}(2000)$	$F_{17}(1990)$
M^{OGE}	1511	1699	1632	1723	2008	1945
Refs. [37, 38]	1535	1745	1670	1715	2025	1955
M^{PDG}	1520 ± 5	1700 ± 50	1675 ± 5	1685 ± 5	2000	1990

In Table IV, we examine the sensitivity of our model to its ingredients by switching off one resonance at a time and noting the χ^2, without further minimizations. As expected, the most

TABLE III: Predicted masses for "missing" negative parity excited baryon by the present work (M^{OGE}) and by Isgur and Karl [37].

	P_{11}	P_{11}	P_{13}	P_{13}	P_{13}	F_{15}
M^{OGE}	1899	2051	1942	1965	2047	1943
Ref. [37]	1890	2055	1955	1980	2060	1955

important role is played by the $S_{11}(1535)$, and the effects of $S_{11}(1650)$ and $D_{13}(1520)$ turn out to be very significant. Within the known resonances, the other two ones contributing largely enough are $F_{15}(1680)$ and $P_{13}(1720)$. In addition to those five known resonances, a new S_{11} appears to be strongly needed by the data, while the smaller effect of a new D_{15} is found non-negligible. Finally, higher mass resonance ($M \gtrsim 2$ GeV) and a new D_{13} do not bring in significant effects.

TABLE IV: The χ^2s shown are the values after turning off the corresponding (known) resonance contribution within the model B, for which $\chi^2 = 2.31$.

Removed N^*	$S_{11}(1535)$	$S_{11}(1650)$	$P_{11}(1440)$	$P_{11}(1710)$	$P_{13}(1720)$	$P_{13}(1900)$
χ^2	162	11.9	2.29	2.39	4.15	2.35
Removed N^*	$D_{13}(1520)$	$D_{13}(1700)$	$D_{15}(1675)$	$F_{15}(1680)$	$F_{15}(2000)$	$F_{17}(1990)$
χ^2	9.83	2.29	2.24	4.82	2.33	2.31
Removed N^*	HM N^*	New S_{11}	New D_{13}	New D_{15}		
χ^2	2.50	12.69	2.63	3.88		

Our model B is built upon resonances given in Table IV. In Table V we investigate possible contributions from the missing resonances (Table III). Here, we add them one by one to the model B, without further minimizations. As reported in Table V, none of them play a noticable role in the reaction mechanism. Please notice that for those resonances we use the masses that we have determined. We have checked the changes of the χ^2 by varying those masses by ± 100 MeV. Moreover, given that there is no unique information available on their widths, we have let them vary between 100 MeV and 1 GeV. The effects of those procedures on the reported χ^2s in Table V come out to be less than 10%.

After having discussed above the s-channel contribution, we end this Section with a few comments. In our models, non-resonant components include nucleon pole term, and u-

TABLE V: The χ^2s shown are the values after adding the corresponding (missing) resonance contribution within model B, for which $\chi^2 = 2.31$.

Added N^*	$P_{11}(1899)$	$P_{11}(2051)$	$P_{13}(1942)$	$P_{13}(1965)$	$P_{13}(2047)$	$F_{15}(1943)$
χ^2	2.31	2.31	2.26	2.31	2.32	2.28

channel contributions, treated as degenerate to the harmonic oscillator shell n. t-channel contributions due to the ρ- and ω-exchanges [45], found [46] to be negligible, are not include in the present work. Our finding about the effect of higher mass resonances being very small, supports the neglect of the t-channel, due to the duality hypothesis (see e.g. Refs. [18, 47]).

Finally, the target asymmetry (T) data [48] are not included in our data base. Actually, those 50 data points bear too large uncertainties to put significant constraints on the parameters [46].

B. Differential cross section and Beam asymmetry

In Figures 1, 2, and 3, we report our results for angular distributions of differential cross sections, excitation functions, and polarized beam asymmetries (Σ), respectively. Results for the models A and B are shown on all three Figures. The first striking point is that model A compares satisfactorily with data up to $W \lesssim 1.65$ GeV, but shows very serious shortcomings above, especially in the range W $\approx$ 1.7 GeV to 1.8 GeV. Model B reproduces the differential cross section and polarization data well enough, though some discrepancies appear at the highest energies and most forward angles ($W \gtrsim 1.85$ and $\theta \lesssim 50°$).

In Fig. 1, we concentrate on the role played by the three most relevant known resonances discussed in Sec.III A (see Table IV), namely, by removing one resonance at a time, within the model B. The $S_{11}(1535)$ is by far the most dominant resonance at lower energies and has sizeable effect up to $W \approx 1.8$ GeV, while the $S_{11}(1650)$ shows significant contributions only at intermediate energies. The $D_{13}(1520)$ has less significant contribution, but its role is crucial in reproducing the correct shape of the differential cross section, especially at intermediate energies.

The importance of the other two known resonances, leading to a significant increase of χ^2 when switched off (see Table IV), are illustrated in the left panel of Fig. 2. While, the $P_{13}(1720)$ affects extreme angles around $W \approx 1.8$ GeV, the $F_{15}(1680)$ is visible only at

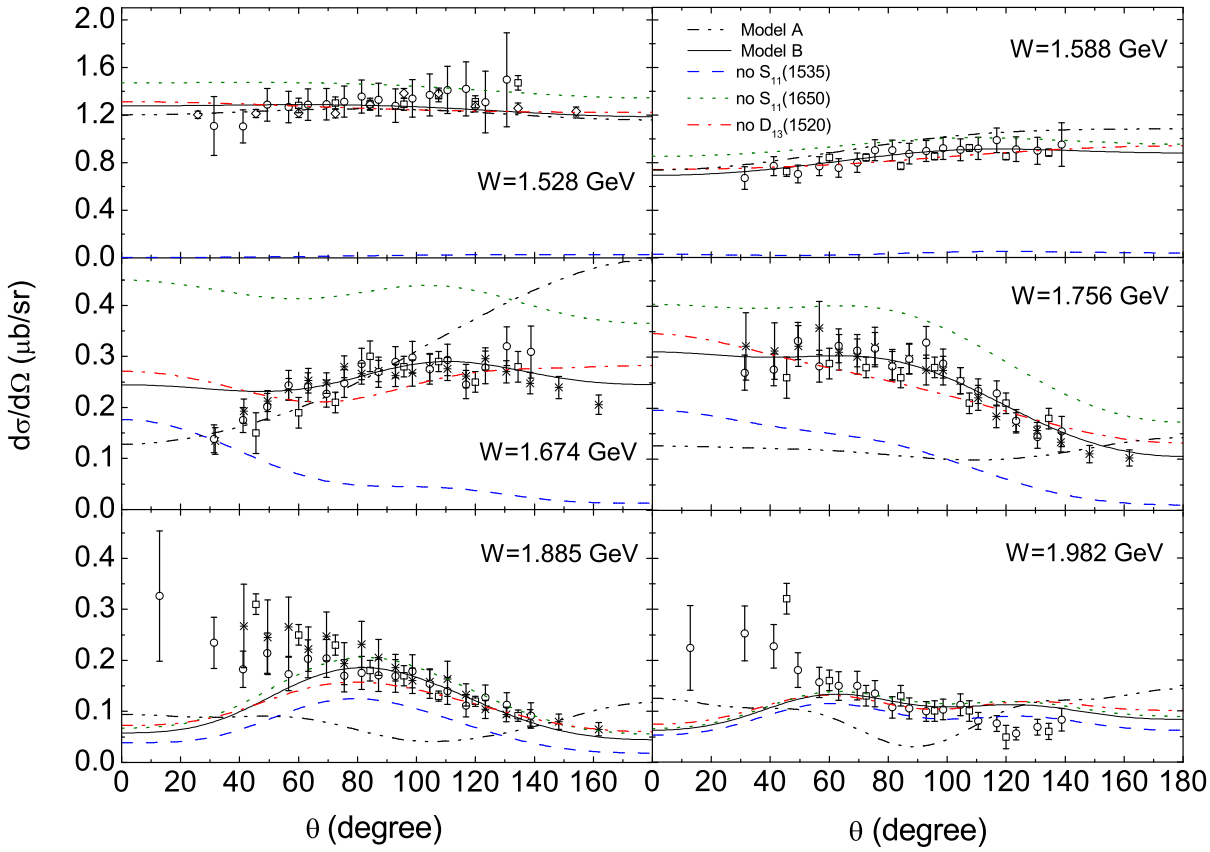

FIG. 1: Differential cross section for the process $\gamma\ p \rightarrow \eta\ p$. The curves are for models A (dash-dot-dotted) and B (full). The other curves are obtained within model B by switching off one resonances at a time: $S_{11}(1535)$ (dashed), $S_{11}(1650)$ (dotted) and $D_{13}(1520)$ (dash-dotted). The data are from CLAS (squares) [2], ELSA (circles) [3], Mainz (diamonds) [1], and GRAAL (stars) [5].

forward angle.

The right panel of Fig. 2 is devoted to the roles played by the three new resonances. As mentioned above, the main shortcoming of the model A appears around $W \approx 1.7$ - 1.8 GeV. This undesirable feature is cured in the model B, due mainly to the new S_{11}, the mass of which turns out to be $M = 1.717$ GeV. Fig. 2 illustrates the increase of χ^2 (Table IV) when that resonance is switched off in the model B. Smaller contributions from the new D_{15} appear in the forward hemisphere, while the new D_{13} has no significant manifestation.

Polarized beam asymmetry results are reported in Fig. 3. As shown in the left panel of that figure, although the model B gives a better account of the data than the model A, the contrast is less important compared to the differential cross-section observable.

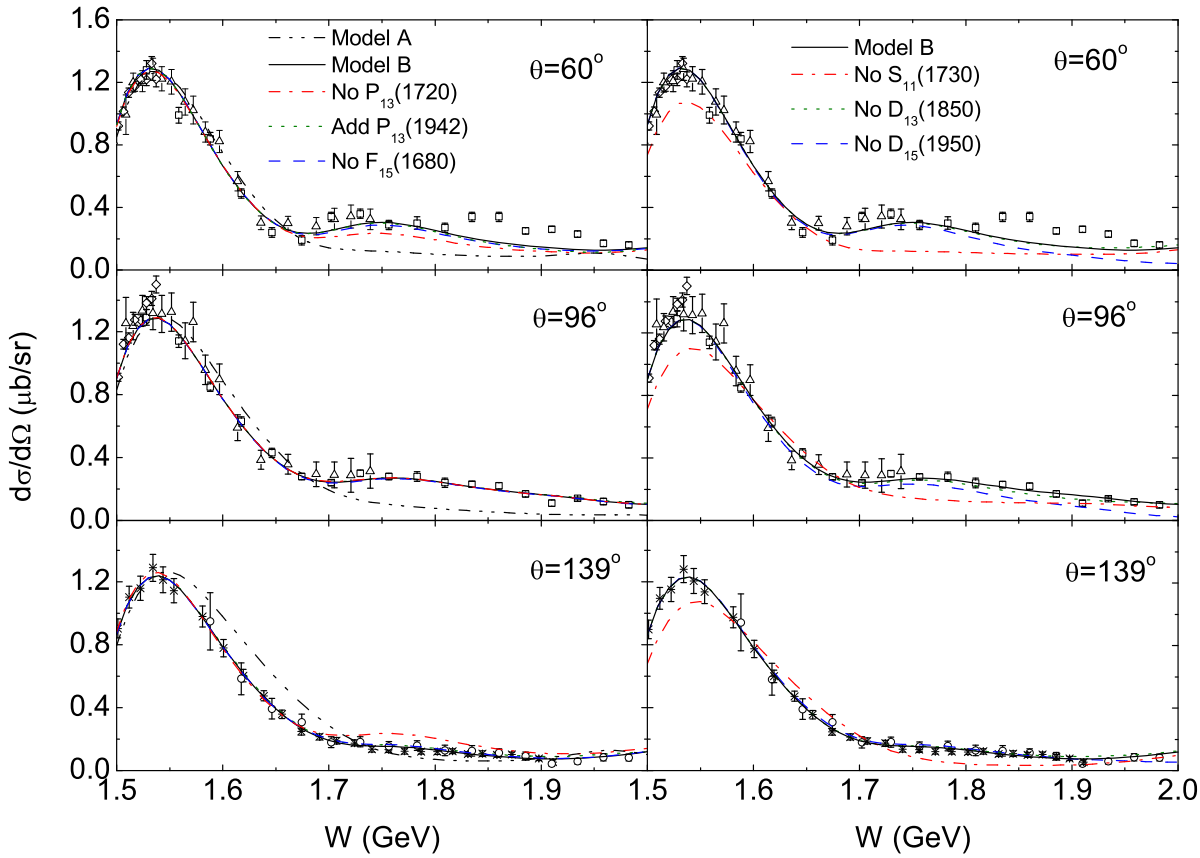

FIG. 2: Differential cross section as a function of W at three angles. The dash-dot-dotted and full curves correspond to the models A and B. All other curves are obtained within the model B by turning off one known resonance or adding a missing one. In the left panel switching off $P_{13}(1720)$ (dash-dotted), $F_{15}(1680)$ (dashed); adding $P_{13}(1942)$ (dotted). In the right panel: switching off $S_{11}(1730)$ (dash-dotted), $D_{13}(1850)$ (dotted), $D_{15}(1950)$ (dashed). The data are from CLAS (squares) [2], Mainz (diamonds) [1], LNS (uptriangles) [4].

The $S_{11}(1535)$ continues playing a primordial role, while the effect of $S_{11}(1650)$ tends to be marginal. This is also the case (middle panel) for the known $P_{13}(1720)$ and missing $P_{13}(1942)$. The established importance of the $D_{13}(1520)$ and $F_{15}(1680)$ (in left and middle panels, respectively) within this observable appear clearly.

In the right panel of Fig. 3, we examine the case of three new resonances. The new S_{11} gives sizeable contributions in the energy range corresponding roughly to its mass. In contrast to the differential cross-section, the new D_{13} appears to be significant in the backward hemisphere. Finally, switching off the new D_{15} improves the agreement with the data at most backward angles shown, while for the cross-section we get an opposite behavior. This

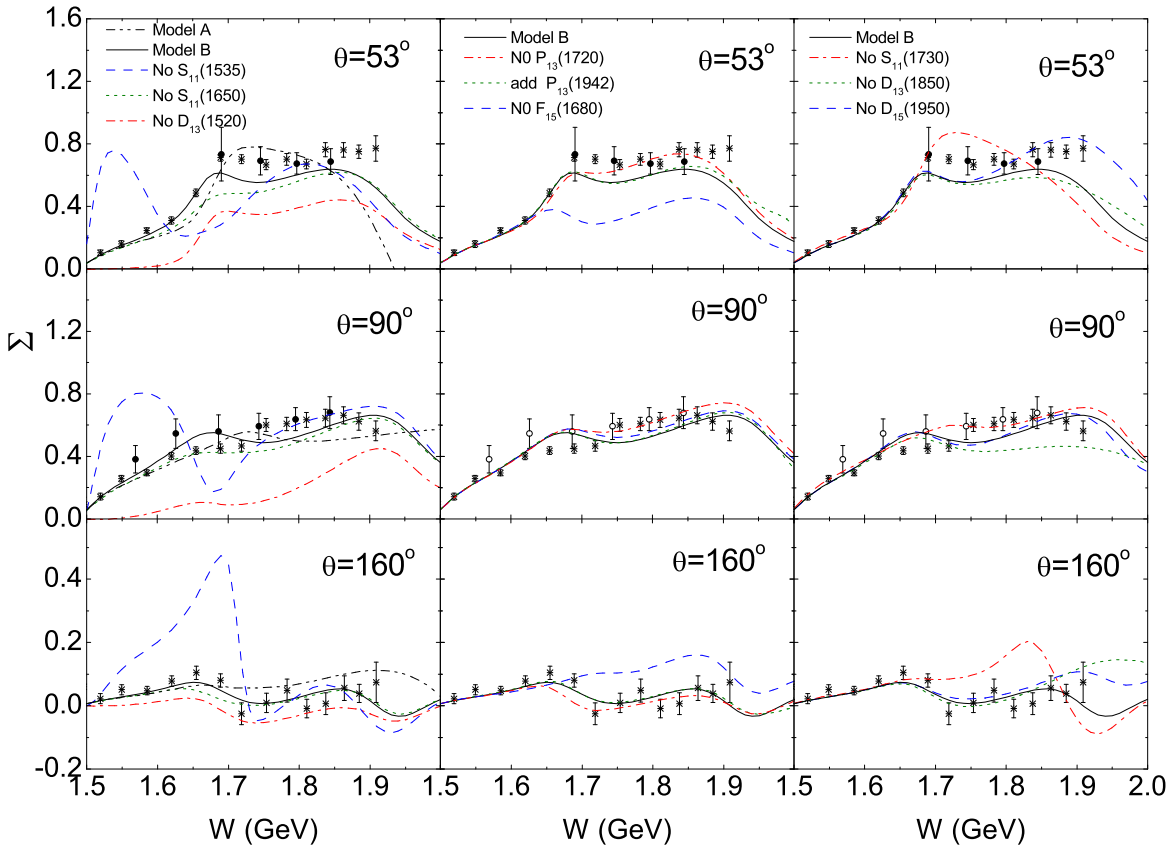

FIG. 3: Polarized beam asymmetry as a function of W. The curves in the left panel are as in Fig. 1, and those in middle and right pannels as in Fig. 2. The data are from ELSA (full circles) [6] and GRAAL (stars) [5].

isolated contradiction reflects the relative weight of data for the two observables (roughly 6 times more differential cross-section data than polarization asymmetry, with comparable accuracies).

This Section, devoted to the observables of the the process $\gamma\, p \to \eta\, p$, in the energy range $W \lesssim 2$ GeV, leads to the conclusion that within our approach, the reaction mechanism is dominated by five known and two new nucleon resonances.

C. Helicity amplitudes and partial decay width

As discussed in Sec. IV (Eqs. (20), (21), and (25)), our approach allows calculating the helicity amplitudes and the partial decay width $N^* \to \eta\, N$ within a given model without further adjustable parameters.

TABLE VI: Helicity amplitudes and decay widths for resonances, with $\Gamma_{\eta N}^{PDG} = \Gamma_{tot} \cdot Br_{\eta N}$ in PDG [42].

Resonances	$A_{1/2}$	$A_{1/2}^{PDG}$	$A_{3/2}$	$A_{3/2}^{PDG}$	$\sigma\sqrt{\Gamma_{\eta N}}$	$(\sigma)\sqrt{\Gamma_{\eta N}^{PDG}}$
$S_{11}(1535)$	72	90 ± 30			7.05	$(+)8.87^{+1.37}_{-1.37}$
$S_{11}(1650)$	60	53 ± 16			-2.20	$1.95^{+0.94}_{-1.57}$
$P_{11}(1440)$	37	-65 ± 4				
$P_{11}(1710)$	27	9 ± 22			1.30	$2.49^{+1.75}_{-0.88}$
P_{11}	3				-1.64	
P_{11}	-2				-0.76	
$P_{13}(1720)$	194	18 ± 30	-72	-19 ± 20	2.07	$2.83^{+1.04}_{-0.71}$
$P_{13}(1900)$	33		1		-0.87	$8.35^{+2.11}_{-2.20}$
P_{13}	32		-2		1.80	
P_{13}	14		2		0.05	
P_{13}	-4		4		-0.73	
$D_{13}(1520)$	-20	-24 ± 9	144	166 ± 5	0.30	$0.51^{+0.07}_{-0.06}$
$D_{13}(1700)$	-6	-18 ± 13	2	-2 ± 24	-0.57	$0.00^{+1.22}_{-0.00}$
$D_{15}(1675)$	-6	19 ± 8	-9	15 ± 9	-1.74	$0.00^{+1.28}_{-0.00}$
$F_{15}(1680)$	14	-15 ± 6	142	133 ± 12	0.44	$0.00^{+1.18}_{-0.00}$
F_{15}	-12		5		0.78	
$F_{15}(2000)$	-1		13		-0.38	
$F_{17}(1990)$	6	1	8	4	-1.25	$0.00^{+2.17}_{-0.00}$

In Table VI we report on our results within the model B, for all n =1 and 2 shell resonances generated by the quark model and complemented with the OGE model. In that Table, 2^{nd} and 4^{th} columns embody our results for the helicity amplitudes. Those amplitudes are in lines with results from other similar approaches (see Tables I and II in Ref. [19]).

Comparing our results for the dominant known resonances of the model B with values reported in PDG [42] (3^{rd} and 5^{th} columns in Table VI) leads to following remarks: *i)* $A_{1/2}$ amplitudes for $S_{11}(1535)$ and $S_{11}(1650)$, as well as $A_{1/2}$ and $A_{3/2}$ for $D_{13}(1520)$ and $A_{3/2}$ for $F_{15}(1680)$ are in good agreement with the PDG values. For this latter resonances the $A_{1/2}$ has the right magnitude, but opposite sign with respect to the PDG value. However,

for that resonance $A_{3/2}$ being much larger than $A_{1/2}$, the effect of this latter amplitude is not significant enough in computing the observables. The amplitudes for $P_{13}(1720)$ deviate significantly from their PDG values, as it is the case in other relevant approaches (see Table II in Ref. [19]). Those large values produced by our model forced us to leave the symmetry breaking coefficient for $P_{13}(1720)$ as a free parameter (Table I) in order to suppress its otherwise too large contribution. As much as other known resonances are concerned we get results compatible with the PDG values for $D_{13}(1700)$ and $F_{17}(1990)$, and to a less extent for $D_{15}(1675)$. For $P_{11}(1440)$ our result deviates significantly from the PDG value. Once again, our result confirms the general trend observed in other works (see Table II in Ref. [19]), which very likely reflects the still unknown structure of that resonance. Finally, we put forward predictions also for the missing resonances, for which we find rather small amplitudes, explaining the negligible roles played by them in our model.

The 6^{th} and 7^{th} columns in Table VI show our results and PDG values, respectively, for the partial decay widths of resonances decay in the ηN channel, where σ is the sign for $\pi\ N \rightarrow\ \eta\ N$ as in Ref. [13]. Notice that the sign (σ) in the PDG is known only for $S_{11}(1535)$. Except for the two star resonance $P_{13}(1900)$, the theoretical results are close to the PDG values.

It is worthwhile noticing that all dominated resonances in our model B have large helicity amplitudes, while some of them turn out to have rather small decay widths to the ηN channel. This result indicates that in looking for appropriate reactions to search for missing resonances it is not enough to have rather sizeable decay width, but one needs to put forward predictions for the observables.

IV. SUMMARY AND CONCLUSIONS

A formalism bringing together a chiral constituent quark approach and one-gluon-exchange model was presented and used to derive photoexcitation helicity amplitudes and partial decay width of the nucleon resonances.

Our approach gives a reasonable account of the measured observables for the process $\gamma\ p\ \rightarrow\ \eta\ p$ from threshold up to $W\ \approx 2$ GeV. Among the twelve nucleon resonances in that energy range, compiled by PDG, five of them are found to play crucial roles in the reaction mechanism, namely, $S_{11}(1535)$, $S_{11}(1650)$, $P_{13}(1720)$, $D_{13}(1520)$, and $F_{15}(1680)$. However,

those known resonances led to our model A, which does not allow an acceptable description of the data. Five extra resonances generated by the formalism, and known as missing resonances, turn out to show no significant contributions to the process under investigation. However, two new resonances reported in the literature, S_{11} and D_{15}, are found relevant to that process; the most important effect comes from the S_{11} resonance. We extracted the mass and width of those resonances: S_{11} [1.730 GeV, 217 MeV], and D_{15} [2.090 GeV, 328 MeV]. Our model B, embodying those latter resonances, describes successfully the data.

The helicity amplitudes and decay widths are calculated with the same parameters. Our results are compatible with other findings and come out close to the PDG values in most cases.

To go further, we are pursing our investigations in two directions,

- In the present work the s-channel resonances with masses above 2 GeV were treated as degenerate, given that the transition amplitudes, translated into the standard CGLN amplitudes were restricted to harmonic oscillator shells $n \leq 2$. recently, we have extended our formalism and derived explicitly the amplitudes also for n= 3 to 6 shells. Model search, including *all* known one to four star resonances in PDG, for $W \approx 2.6$ GeV is in progress [46].

- Our constituent quark approach applied to the $\gamma\, p \rightarrow K^+\Lambda$ channel [49], showed that the intermediate meson-baryon states, treated within a coupled channel formalism [50], have significant effects on the photoproduction observables [31]. A more sophisticated coupling-channel treatment [51] has been developed and is being applied to the η photoproduction reaction. Results of that work will be reported elsewhere.

Acknowledgements

We are deeply grateful to Qiang Zhao for enlightening discussions.

APPENDIX A: MIXING COEFFICIENTS OF THE WAVE FUNCTIONS

In Table VII, we present the mixing coefficients of the wave functions. In Ref. [36, 37], Isgur and Karl have given their explicit values for positive parity and negative parity

resonances respectively. But in Ref. [36] the mixing between $n = 0$ and $n = 2$ shells is not considered. Such mixings for the ground state are given in Ref. [13] without the contribution of ^2P_A. The parameters in that reference are determined only by the mass spectrum. Here we give our results by fitting both the mass spectrum and the η photoproduction observables. In calculation we follow the conventions in Ref. [13].

The mixing coefficients reported here lead to mixing angles, Θ_S = -31.7° and Θ_D = 6.4° in agreement with results from other authors [52–55].

TABLE VII: Mixing coefficients of the wave functions.

state	wave function($^{2S+1}L_\pi$)				
S11	^2P_M	^4P_M			
N(1535)	-0.851	0.526			
N(1650)	0.526	0.851			
P11	^2S_S	^4D_M	^2P_A	$^2S'_S$	^2S_M
N(938)	0.941	-0.043	-0.002	-0.260	-0.211
N(1440)	0.268	0.000	0.000	0.964	0.006
N(1710)	0.175	-0.343	-0.071	-0.054	0.919
	-0.103	-0.839	-0.424	0.031	-0.324
N(2100)	-0.032	-0.421	0.903	0.010	-0.080
P13	^2D_S	^2D_M	^4D_M	^2P_A	^4S_M
N(1720)	0.858	-0.483	0.023	-0.003	-0.176
N(1900)	0.314	0.234	-0.365	0.095	0.839
	-0.185	-0.482	0.606	-0.333	0.505
	0.359	0.686	0.496	-0.387	-0.065
	-0.059	-0.096	-0.502	-0.854	-0.073
D13	^2P_M	^4P_M			
N(1520)	-0.994	-0.111			
N(1700)	-0.111	0.994			
D15	^4P_M				
N(1675)	1.000				
F15	^2D_S	^2D_M	^4D_M		
N(1680)	0.883	-0.469	0.001		
	-0.457	-0.860	-0.225		
N(2000)	-0.107	-0.198	0.974		
F17	^4D_M				
N(1990)	1.000				

[1] B. Krusche et al., Phys. Rev. Lett. **74**, 3736 (1995).

[2] M. Dugger *et al.* (CLAS Collaboration), Phys. Rev. Lett. **89**, 222002 (2002).

[3] V. Crede *et al.* (CB-ELSA Collaboration), Phys. Rev. Lett. **94**, 012004 (2005).

[4] T. Nakabayashi *et al.*, Phys. Rev. C **74**, 035202 (2006).

[5] O. Bartalini *et al.* (GRAAL Collaboration), Eur. Phys. J. A **33**, 169 (2007).

[6] D. Elsner *et al.* (CB-ELSA and TAPS Collaborations), Eur. Phys. J. A **33**, 147 (2007).

[7] W.-T. Chiang, S. N. Yang, L. Tiator, M. Vanderhaeghen, and D. Drechsel, Phys. Rev. C **68**, 045202 (2003).

[8] T. Feuster and U. Mosel, Phys. Rev. C **59**, 460 (1999).

[9] A. V. Anisovich, A. Sarantsev, O. Bartholomy, E. Klempt, V. A. Nikonov, and U. Thoma, Eur. Phys. J. A **25**, 427 (2005); A. V. Sarantsev, V. A. Nikonov, A. V. Anisovich, E. Klempt, and U. Thoma, Eur. Phys. J. A **25**, 441 (2005).

[10] R. A. Arndt, W. J. Briscoe, I. I. Strakovsky, and R. L. Workman, Int. J. Mod. Phys. **A22**, 349 (2007).

[11] L. A. Copley, G. Karl, and E. Obryk, Nucl. Phys. **B13**, 303 (1969).

[12] R. P. Feynman, M. Kislinger, and F. Ravndal, Phys. Rev. D **3**, 2706 (1971).

[13] R. Koniuk and N. Isgur, Phys. Rev. D **21**, 1868 (1980); Erratum *ibid* **23**, 818 (1981).

[14] S. Capstick, Phys. Rev. D **46**, 2864 (1992).

[15] Z. Li, H. Ye, and M. Lu, Phys. Rev. C **56**, 1099 (1997).

[16] A. Manohar and H. Georgi, Nucl. Phys. **B234**, 189 (1984).

[17] Z. Li and B. Saghai, Nucl. Phys. **A644**, 345 (1998).

[18] B. Saghai and Z. Li, Eur. Phys. J. A **11**, 217 (2001); B. Saghai and Z. Li, *Proceedings of NSTAR 2002 Workshop on the Physics of Excited Nucleons*, Pittsburgh, PA (USA), 2002; Editors S.A. Dytman and E.S. Swanson (World Scientific, New Jersey, 2003), arXiv: nucl-th/0305004.

[19] S. Capstick and W. Roberts, Prog. Part. Nucl. Phys. **45**, 5241 (2000), and references therein.

[20] R. Bijker, F. Iachello, and A. Leviatan, Ann. Phys. **236**, 69 (1994); *ibid* **284**, 89 (2000), and references therein.

[21] M. M. Giannini, E. Santopinto, and A. Vassallo, Eur. Phys. J. A **12**, 447 (2001); *Proceedings*

of NSTAR 2002 Workshop on the Physics of Excited Nucleons, Pittsburgh, PA (USA), 2002; Editors S. A. Dytman and E. S. Swanson, World Scientific (2003), arXiv: nucl-th/0302019.

[22] Z. Li and R. Workman, Phys. Rev. C **53**, R549 (1996).

[23] M. Batinic, I. Dadic, I. Slaus, A Svarc, and B. M. K. Nefken, arXive: nucl-th/9703023.

[24] M. M. Giannini, E. Santopinto, and A. Vassallo, Eur. Phys. J. A **12**, 447 (2001).

[25] J.-Z. Bai *et al.* (BES Collaboration), Phys. Lett. **B510**, 75 (2001); M. Ablikim *et al.* (BES Collaboration), arXiv: hep-ex/0405030; B. S. Zou (BES Collaboration), *Proceeding of the Workshop on the Physics of Excited Nucleons, Grenoble*, France, 2004; Editors J.-P. Bocquet, V. Kuznetsov, and D. Rebreyend, World Scientific (2004); Sh. Fang (BES Collaboration), arXiv: hep-ex/0509034.

[26] G.-Y Chen, S. Kamalov, S. N. Yang, D. Drechsel, and L. Tiator, Nucl. Phys. **A723**, 447 (2003).

[27] W. T. Chiang, S. N. Yang, M. Vanderhaeghen, and D. Drechsel, Nucl. Phys. **A723**, 205 (2003).

[28] V. A. Tryasuchev, Eur. Phys. J. A **22**, 97 (2004).

[29] T. Mart, A. Sulaksono, and C. Bennhold, arXiv: nucl-th/0411035.

[30] N. G. Kelkar, M. Nowakowski, K. P. Khemchandani, and S. R. Jain, Nucl. Phys. **A730**, 121 (2004).

[31] B. Juliá-Díaz, B. Saghai, T.-S. H. Lee, and F. Tabakin, Phys. Rev. C **73**, 055204 (2006).

[32] G. F. Chew, M. L. Goldberger, F. E. Low, and Y. Nambu, Phys. Rev. 106, 1345 (1957).

[33] R. L. Walker, Phys. Rev. **182**, 1729 (1969).

[34] V. Chaloupka, *et al.* (Particle Data Group), Phys. Lett. **B50**, 1 (1974).

[35] R. G. Moorhouse, Phys. Rev. Lett. **16**, 772 (1966).

[36] N. Isgur and G. Karl, Phys. Lett. **B74**, 353 (1978).

[37] N. Isgur and G. Karl, Phys. Rev. D **19**, 2653 (1979).

[38] N. Isgur and G. Karl, Phys. Rev. D **18**, 4187 (1978).

[39] L. Y. Glozman and D. O. Riska, Phys. Rep. **268**, 263 (1996).

[40] J. He and Y.-b. Dong, , Nucl. Phys. **A725** 201 (2003).

[41] F. Wang, J.-L. Ping, H.-R. Pang, and J. T. Goldman, Mod. Phys. Lett. **A18**, 356 (2003).

[42] W. M. Yao *et al.* (Particle Data Group), J. Phys. G **33**, 1 (2006).

[43] S. Capstick and W. Roberts, Phys. Rev. D **49**, 4570 (1994).

[44] B. S. Zou, Nucl. Phys. **A790**, 110 (2007).

[45] M. Benmerrouche, N. C. Mukhopadhyay, and J. F. Zhang, Phys. Rev. D **51**, 3237 (1995).

[46] J. He, B. Saghai, Z. Li, Q. Zhao, and J. Durand, *Proceeding of NStar2007 Workshop*, Sept. 2007, Bonn (Germany), to appear in Eur. Phys. J. A, arXiv: 0710.5677 (nucl-th); comprehensive paper in preparation.

[47] P. Collins, *An Introduction to Regge Theory and High Energy Physics*, (Cambridge University Press, 1977); B. Saghai and F. Tabakin, Phys. Rev. C **53**, 66 (1996).

[48] A. Bock *et al.*, Phys. Rev. Lett. **81**, 534 (1998).

[49] B. Juliá-Díaz, B. Saghai, F. Tabakin, W. T. Chiang, T.-S. H. Lee, and Z. Li, Nucl. Phys. **A755**, 463 (2005).

[50] W.-T. Chiang, B. Saghai, F. Tabakin, and T.-S. H. Lee, Phys. Rev. C **69**, 065208 (2004).

[51] J. Durand, B. Juliá-Díaz, T.-S.H. Lee, B. Saghai, and T. Sato, to be submitted for publication.

[52] N. Isgur and G. Karl, Phys. Lett. **B72**, 109 (1977); N. Isgur, G. Karl, and R. Koniuk, Phys. Rev. Lett. **41**, 1269 (1978).

[53] J. Chimza and G. Karl, Phys. Rev. D **68**, 054007 (2003).

[54] S. Capstick and W. Roberts, Fizika **B13**, 271 (2004).

[55] I. K. Bensafa, F. Iddir, and L. Semalala, arXiv: hep-ph/0511195.